Environmental Health Perspectives
Vol. 12, pp. 81–88, 1975

Blood-Brain Barrier Dysfunction in Acute Lead Encephalopathy: A Reappraisal

by Thomas W. Bouldin,* Paul Mushak,* Lorcan A. O'Tuama,† and Martin R. Krigman*

Acute lead encephalopathy was induced in adult guinea pigs by administering daily oral doses of lead carbonate. During the development of the encephalopathy, the structural and functional integrity of the blood–brain barrier was evaluated with electron microscopy and tracer probes. Blood, cerebral gray matter, liver, and kidney were analyzed for lead, calcium, and magnesium content.

The animals regularly developed an encephalopathy after four doses of lead. There were no discernible pathomorphologic alterations in the cerebral capillaries or perivascular glial sheaths. Furthermore, no evidence of blood–brain barrier dysfunction was demonstrated with Evans blue–albumin complex or horseradish peroxidase. Blood–brain barrier permeability to radiolead was not increased in the intoxicated animals. During the development of the encephalopathy there was a progressive rise in the lead concentration in all tissues. Concurrently, there was a significant rise in brain calcium.

These results suggest that the encephalopathic effects of lead may be mediated directly at the neuronal level.

Introduction

The vulnerability of the nervous system to lead is well known; however, the pathogenesis of lead encephalopathy remains a vexing problem. Based upon clinical and experimental studies, a number of investigators (*1–6*) have concluded that the encephalopathic effects of lead are mediated through a primary vascular lesion and a concomitant blood–brain barrier dysfunction. This conclusion is based upon the presence of electron-dense vacuoles in perivascular astrocytic end-feet and endothelial hyperplasia in experimental and clinical cases of lead encephalopathy (*3, 5*). Moreover, perivascular hemorrhages, cerebral edema, and blood–brain barrier dysfunction as evaluated by macromolecular tracers are prominent features of the encephalopathy in the suckling rat model of Pentschew and Garro (*2, 3*). Despite the existence of these cerebral vascular alterations in lead intoxication, the direct neural effects of lead must also be considered as a factor in the pathogenesis of lead encephalopathy. Evidence is accumulating that lead ions can directly affect synaptic transmission (*7*). Moreover, it has been previously shown that when lead ions are directly instilled into the cerebrospinal fluid of dogs, the animals develop an encephalopathy and ultimately die (*8, 9*).

*Department of Pathology, University of North Carolina, School of Medicine, Chapel Hill, N.C. 27514.

†Department of Neurology, University of North Carolina, School of Medicine, Chapel Hill, N. C. 27514.

We report here studies designed to evaluate the role of blood–brain barrier dysfunction in the genesis of acute lead encephalopathy in the adult guinea pig. The model used was initially described by Popow (*10*) in 1885 and more fully by Weller (*11*) in 1927. Four consecutive daily oral doses of lead carbonate (155 mg) produce an encephalopathy in the adult guinea pig characterized by tonic-clonic seizures. When five consecutive daily doses of lead are given, all of the animals develop seizures and die. Despite the development of this severe encephalopathy, these animals show no morphological changes in the structures of the blood–brain barrier, and the permeability of the barrier to macromolecules is not increased.

Materials and Methods

Experimental Model

Random-bred, adult, male guinea pigs, weighing 475–800 g, were maintained in individual plastic cages with an ambient temperature of 68°F, 12 hr of artificial light per day, and fed guinea pig chow and tap water, *ad libitum*. A single, daily, oral dose of 155 mg of lead carbonate in a gelatin capsule was administered to the experimental animals. [The dosage is arbitrary and was used by Weller (*11*) because it produced an encephalopathy.]

Morphologic Evaluation of Blood–Brain Barrier with Evans Blue and Horseradish Peroxidase

The guinea pigs were sacrificed 24 hr after two (three animals), three (four animals), five (six animals), or six (two animals) consecutive daily doses. Two of the five-dose animals also received Evans blue (5 mg/ml saline), intraperitoneally, 24 hr prior to sacrifice. After pentobarbital anesthesia (3.6 mg/100 g body weight, intramuscularly), the animals received an intravascular injection of Sigma type II horseradish peroxidase (25 mg/100 g body weight, dissolved in 3 ml physiologic saline) and were sacrificed 10–15 min later by decapitation or intravascular perfusion. For perfusion, the animals were mechanically ventilated while the thorax was opened and the ascending aorta was cannulated via the heart. The brains were perfused with Karnovsky's dialdehyde fixative (*12*) diluted (1:3) with 0.1*M* sodium cacodylate buffer (pH 7.4) for 15 min at a pressure of 100 cm of fixative. The perfused brains and the brains from the decapitated animals were removed, coronally sectioned through the neostriatum, mamillary bodies, and midbrain and cerebellum, and fixed by immersion for 2–4 hr at room temperature in full strength Karnovsky's fixative. These fixed tissues were then washed overnight in 0.1*M* sodium cacodylate buffer, pH 7.2, at 4°C. For light microscopy, 20 μm coronal sections of brain were cut with a freezing microtome; for electron microscopy, 70 μm slices of cerebral cortex and cerebellum were cut with a Smith-Farquhar tissue chopper. Peroxidase activity in the frozen sections and tissue slices was identified by using the method of Graham and Karnovsky (*13*). Frozen sections were also mounted in glycerol for the identification of Evans blue by fluorescence microscopy. Following incubation in the Graham-Karnovsky medium, the 70 μm slices were postfixed in 1% osmium tetroxide in 0.1*M* cacodylate buffer for 1 hr, stained *en bloc* with 1% uranyl acetate in 0.1 *M* maleate at pH 5.4 for 1 hr, dehydrated with graded ethanol and finally with propylene oxide, and embedded in Epon 812. Survey thick sections were stained with toluidine blue. Ultrathin sections, either unstained or doubly stained with uranyl acetate and lead citrate, were examined in a JEM-T7 electron microscope. Brain tissue was also prepared for conventional light microscopy by embedding in paraffin, sectioning at 6–8 μm, and staining with hematoxylin and eosin or Luxol fast blue-periodic acid-Schiff stains.

Control guinea pigs did not receive lead carbonate, but did receive intravascular horseradish peroxidase 15 min prior to vascular brain perfusion. Tissue was processed for light and electron microscopy as previously described.

Penetration of Tracer Amounts of Radioactive Lead (^{210}Pb) into Brain

The methodology is as previously described elsewhere (*14*). In brief, control and experimental groups of animals were prepared as described above under experimental methods. ^{210}Pb (in approximately 3*N* HNO_3; 60 mCi/mg of lead), 0.01 mCi/kg, was injected into a cannula inserted in the internal jugular vein. Blood samples were taken at 5, 60, 120, and 240 min after the tracer injection. The samples were diluted with saline to 1 ml and counted for ^{210}Pb. Blood samples of 0.5 ml were taken for total lead estimation.

Tissue Analyses for Lead, Calcium, and Magnesium

Lead-treated guinea pigs were sacrificed by decapitation 24 hr after one (four animals), three (four animals), and five (three animals) doses of lead; four control animals were also studied. Blood, cerebral gray matter, liver, and kidney were analyzed for lead, calcium, and magnesium. Tissue homogenates and whole blood were analyzed for lead by the Delves cup microabsorption spectrophotometric technique (*15*) as modified by Ediger and Coleman (*16*). The samples were analyzed directly without predigestion in a Perkin-Elmer atomic absorption spectrophotometer equipped with a deuterium arc. Calcium and magnesium were also measured by atomic absorption spectroscopy. Each of the values reported is the average of three sample determinations.

Results

The guinea pigs began showing symptoms of intoxication after two to three doses of lead. These symptoms included an increased startle response and decreased food consumption. By the fifth dose the animals were obtunded, with a greatly increased startle response, and occasional seizures. Tonic-clonic seizures occurred in three of the animals studied for morphologic alterations in the blood–brain barrier. Examination of the histologic preparations by light microscopy revealed no demonstrable changes in the central nervous system. There were also no signs of hemorrhage.

Macromolecular Tracer Studies

Macroscopic examination of the brains of lead-poisoned animals revealed no abnormal staining of the neural tissue by Evans blue. By fluorescence and light microscopy, the red fluorescence of the Evans blue and the brown reaction product of the horseradish peroxidase were limited to the vascular lumina except for the choroid plexus and tuber cinereum—areas which normally have no blood–brain barrier to these macromolecules (Fig. 1).

By electron microscopy, the capillary endothelium of lead-poisoned animals (Fig. 2) was indistinguishable from that of control animals. The endothelial cells had a normal complement of organelles and no increased numbers of vacuoles or pinocytotic vesicles. The perithelial cells, basement membranes, and perivascular glial end-feet were normal in the lead-poisoned animals. Intracellular and extracellular edema were not apparent at any time in the intoxicated animals. The electron-dense reaction product was limited to capillary lumina (Fig. 3), and did not extend beyond interendothelial cell zonulae occludentes. Reaction product was not observed within pericapillary basement membranes or the extracellular space of the brain. Examination of the choroid plexus revealed reaction product within capillary lumina, perivascular stroma, and in the lateral intercellular spaces between choroidal epithelial cells (Fig. 4). Reaction product did not pass through choroidal epithelial zonulae occludentes to the ventricular surface.

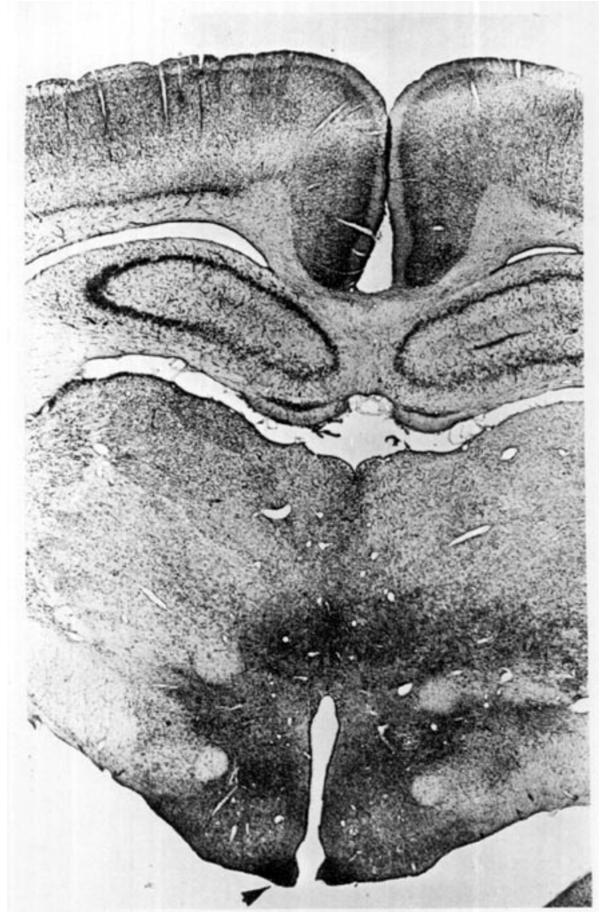

FIGURE 1. Macrophotograph of coronal section of brain from animal receiving 5 daily doses of lead and a single intravascular injection of horseradish peroxidase (HRP) 15 min prior to sacrifice. Reaction product of HRP is limited to the neuropil of the tuber cinereum (arrow). Nissl stain. × 14.

Radiolead Levels in Blood and Brain

Constant levels of ^{210}Pb were achieved in blood and brain within 5 min of intravenous injection of radiolead. Despite a 13-fold increase in total blood lead and a 3-fold increase in total brain lead levels in the encephalopathic animals, the concentration of ^{210}Pb in whole brain was not significantly different in the two groups (Table 1). Levels of ^{210}Pb

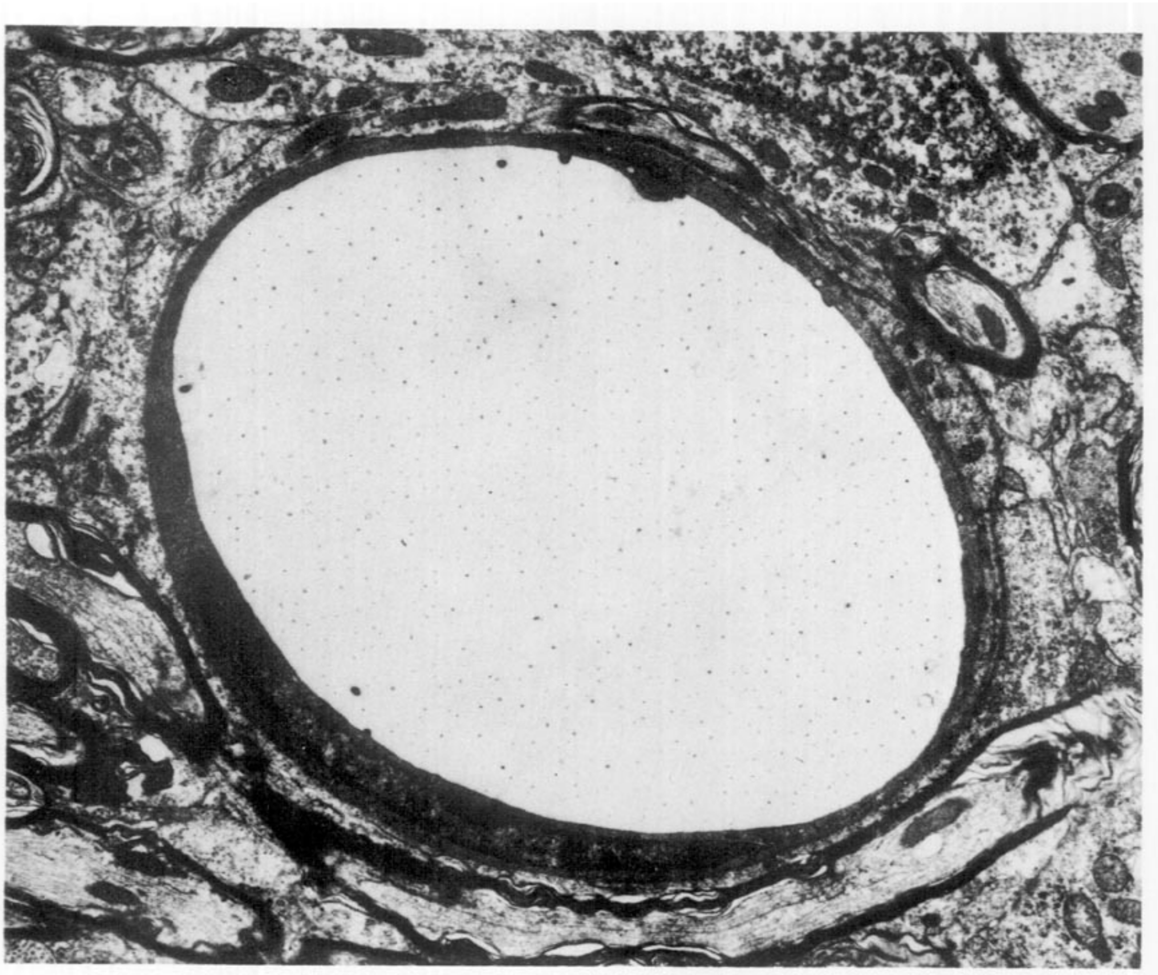

FIGURE 2. Electron photomicrograph of cerebellar capillary from animal receiving five daily doses of lead and a single intravascular dose of HRP 15 min prior to perfusion-fixation. There is no evidence of reaction product in the capillary basement membrane or surrounding extracellular space. The capillary endothelium and surrounding neuropil show no pathomorphologic alterations. Particulate material within vascular lumen is a perfusion artifact. Uranyl acetate and lead citrate. ×9500.

in cerebellum in control and in poisoned animals averaged 1.5 times those found in whole brain.

Table 1. Total and radioactive lead in blood and brain 5 min after pulse injection (0.01mCi/kg ^{210}Pb IV).[a]

	Blood lead, μg/g	Brain: Lead, μg/g	Brain: Radiolead (^{210}Pb), cpm/g
Control	10.54 ± 1.77 (5)	0.26 ± 0.03 (6)	89 ± 26 (9)
Lead-poisoned	132.74 ± 40.8 (7)	0.72 ± 0.10 (4)	116 ± 105 (3)

[a]Values indicate means ± S. D. Numbers of experiments are in parentheses.

Tissue Analysis for Lead, Calcium, and Magnesium

The results of these tissue analyses are presented in Table 2. There was a progressive rise in lead concentration in all of the tissues analyzed. This rise was most marked after the fifth lead dose, particularly in the cerebral gray matter. Cerebral tissue also accumulated calcium and magnesium during the course of the lead intoxication. In contrast, the calcium and magnesium blood levels were constant throughout this interval. The liver and kidney level of these cations varied in no definable pattern but the variance rose. This may indicate an early perturbation in calcium metabolism.

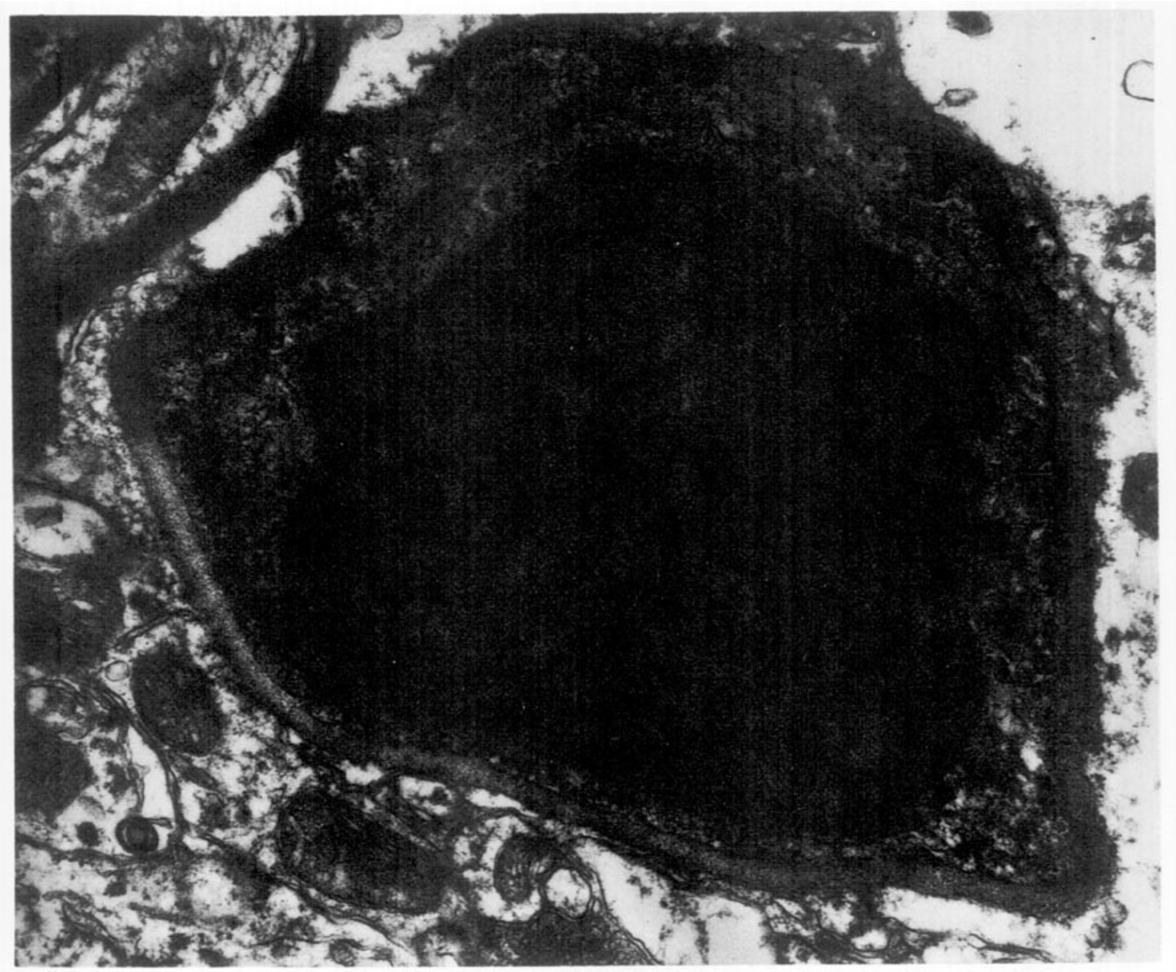

FIGURE 3. Electron photomicrograph of cerebellar capillary from animal receiving five daily doses of lead, and a single intravascular dose of HRP 15 min prior to sacrifice. Fixation was by immersion. HRP reaction product is limited to the vascular lumen and is not present within the basement membrane or surrounding extracellular space. Uranyl acetate and lead citrate. ×30,000.

Discussion

We found no morphologic or functional evidence of an altered blood–brain barrier in lead-poisoned guinea pigs. The structure of the cerebral capillary endothelium, basement membrane, and perivascular glial sheath in poisoned animals was indistinguishable from that found in controls. This morphologic evidence for the integrity of the blood–brain barrier in acute lead encephalopathy was strongly supported by the failure of the macromolecules horseradish peroxidase and Evans blue–albumin complex to pass beyond the cerebral capillary endothelium or the zonulae occludentes of the choroidal epithelium (*17*). The absence of cerebral edema as evaluated morphologically, further supports the existence of an intact blood–brain barrier.

These observations indicate that convincing clinical and chemical lead encephalopathy can occur without any demonstrable change in blood–brain barrier morphology or permeability. The findings are therefore inconsistent with the suggestion that lead induces an encephalopathy through a primary vascular alteration as postulated by Pentschew and others (*1–6*). The absence of vascular alterations in lead-poisoned guinea pigs contrasts sharply with the prominent vascular lesions in lead-poisoned suckling rats. Since these vascular lesions can only be induced in suckling rats during the first 2 weeks of life (M. R. Krigman, unpublished results), one might theorize that the

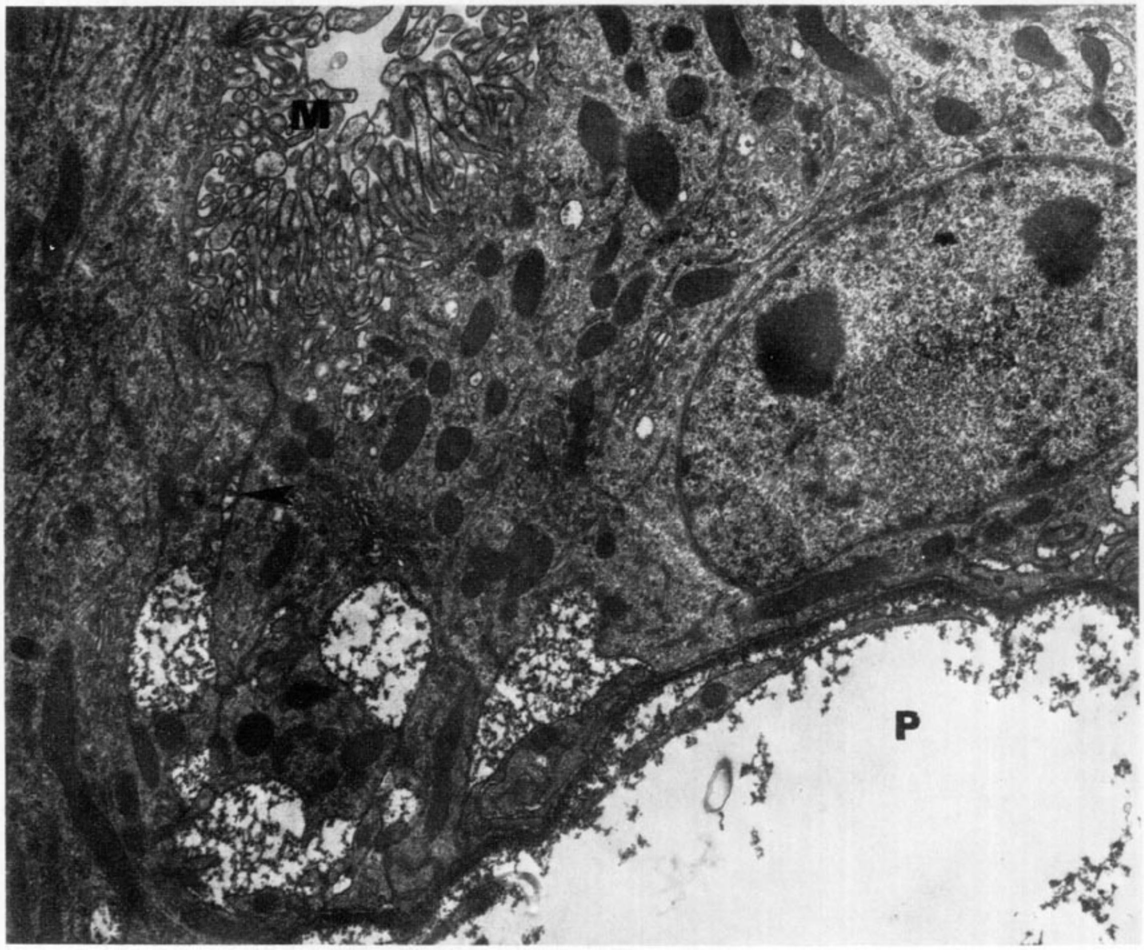

FIGURE 4. Choroid plexus from animal receiving five daily doses of lead and a single intravascular dose of HRP 15 min prior to perfusion-fixation. The floccular HRP reaction product is present within the pericapillary stroma (P) and lateral intercellular space (arrow) between two choroidal epithelial cells, but is not present on the microvilli (M) projecting into the ventricle. Uranyl acetate and lead citrate. ×11,000.

immature, proliferating capillaries of the suckling rat are vulnerable to the toxic effects of lead. Supporting this thesis is the recent observation that significant capillary endothelial cell damage also occurs in the developing chick embryo exposed to lead (*18*). These contrasting data from different animal models suggest that in acute lead poisoning one can delineate within the central nervous system two *loci minoris resistentiae*: the neuron and the proliferating endothelial cell.

The adult guinea pig model of lead encephalopathy has much in common with the acute encephalopathy of man. The symptomatology of the lead-poisoned guinea pigs closely resembles the obtundation and seizures noted in humans with acute lead encephalopathy. Although the pathomorphologic changes in the guinea pig brains are minimal and nonspecific, such minimal changes are occasionally the only pathologic findings in human cases of acute lead encephalopathy. As emphasized by Pentschew (*1*), cerebral edema is not invariably associated with human lead encephalopathy. In 20 necropsied cases of human lead encephalopathy reviewed by Pentschew, only six had a conspicuous increase in brain volume and three had no gross or microscopic brain changes (*1*).

By arguing against a primary vasculopathy in lead encephalopathy, our results must revive the hypothesis that the encephalopathic effects of lead

Table 2. Tissue concentration of metals in selected organs during the course of lead intoxication.

Tissue	No. of doses of lead[a]	Metal level, μg/g wet weight[b]		
		Lead	Calcium	Magnesium
Cerebral gray matter	0	0.17 ± 0.12	0.91 ± 0.55	1.8 ± 0.61
	1	0.59 ± 0.23	1.3 ± 0.43	2.0 ± 0.52
	3	1.3 ± 0.62	1.5 ± 0.51	2.4 ± 0.71
	5	3.8 ± 1.8	1.6 ± 0.60	2.3 ± 0.56
Kidney	0	5.8 ± 2.1	1.8 ± 0.20	1.6 ± 0.04
	1	73 ± 14	1.3 ± 0.30	1.3 ± 0.13
	3	137 ± 48	1.3 ± 0.24	1.3 ± 0.22
	5	556 ± 51	1.2 ± 0.20	1.8 ± 0.62
Liver	0	2.1 ± 1.8	1.2 ± 0.03	1.2 ± 0.06
	1	49 ± 2.1	1.2 ± 0.33	1.0 ± 0.22
	3	65 ± 41	1.2 ± 0.13	1.3 ± 0.10
	5	132 ± 34	2.1 ± 1.2	1.6 ± 0.61
Blood	0	0.08 ± 0.02	42.0 ± 0.94	6.2 ± 0.40
	1	0.61 ± 0.16	43 ± 0.64	6.0 ± 0.28
	3	1.3 ± 0.74	43 ± 0.55	5.7 ± 0.46
	5	1.6 ± 0.62	43 ± 0.44	5.8 ± 0.24

[a]Lead carbonate, 155 mg oral dose.
[b]Metal level in blood, μg/ml.

are mediated at the neuronal level. Recent studies demonstrate fundamental neural alterations directly induced by lead. Bull et al. (*19*) reported that lead chloride interferes with the potassium-stimulated respiration of rat cerebral cortex slices, and Nathanson et al. (*20*) found that even low concentrations of lead inhibit brain adenyl cyclase *in vitro*. Lead has also been found (*7*) to inhibit competitively the calcium-mediated release of neurotransmitters from presynaptic nerve terminals of the bullfrog sympathetic ganglia studied *in vitro*.

The radiolead data show that, although the net flux of lead across the blood–brain barrier is increased in lead encephalopathy, the permeability coefficient of ^{210}Pb is approximately the same in control and poisoned animals. This indicates that acute lead poisoning does not reveal a saturable process which might serve to limit lead uptake in the face of acute overdosage. This conclusion is supported by the failure of lead encephalopathy to produce structural changes in the cerebral capillary–glial complex which is the putative site of carrier-dependent passage of small molecules from blood into brain. Our findings leave open for further study two important and related problem areas: (a) the forces governing unidirectional uptake of tracer amounts of lead in the normal brain and (b) the possible effects of lead poisoning on the metabolism and transport of other physiologically important cations such as calcium and magnesium.

Some information on the latter issue is provided by the elevated brain calcium and magnesium levels found in the poisoned animals. Hoffman and Weber (*21*) have also reported elevated brain calcium levels in lead-poisoned rats, even after a single dose of lead and after parathyroidectomy. Unfortunately, these investigators did not measure magnesium levels. While the mechanisms for the progressive rise in these cations are unknown, the accumulation of calcium may be related to an altered transport system. From *in vitro* experiments it appears that calcium enters the central nervous system passively and is transported out actively (*22*). The progressive accumulation of brain calcium observed in this study in the presence of a constant blood level suggests the efflux of this cation may be reduced due to a disturbance of an active efflux mechanism for calcium. An alternative possibility is competition by lead for binding sites on molecules involved in the active efflux of calcium from the brain. The recent report of lead-induced inhibition of adenyl cyclase is of special interest because of the close interrelationship between cyclic adenosine 3′,5′-monophosphate and calcium (*23*).

In summary, we have demonstrated that lead can enter the central nervous system and produce a severe and fatal encephalopathy in the adult guinea pig without morphologic alterations of the blood–brain barrier or demonstrable dysfunction of this barrier to macromolecules. Thus in this experimental model the encephalopathic effects of lead may well be directly mediated at the cellular level. This does not mean that lead does not produce a vasculopathy in susceptible species. We do, however, raise the question as to how much such vascular lesions contribute to the acute encephalopathy associated with lead intoxication.

Acknowledgement

This study was supported by U.S. Public Health Service Grant ES01104-01.

REFERENCES

1. Pentschew, A. Morphology and morphogenesis of lead encephalopathy. Acta Neuropathol. (Berl.) 5: 133 (1965).
2. Pentschew, A., and Garro, F. Lead encephalo-myelopathy of the suckling rat and its implications on the porphyrinopathic nervous diseases. Acta Neuropathol. (Berl.) 6: 266 (1966).
3. Lampert, P., Garro, F., and Pentschew, A. Lead encephalopathy in suckling rats. In: Symposium on Brain Edema, Vienna, 1965. I. Klatzo and F. Seitelberger, eds. Springer Verlag, Berlin-Heidelberg-New York, 1967.
4. Thomas, J. A., Dallenbach, F. D., and Thomas, M. Considerations on the development of experimental lead encephalopathy. Virchows Arch. (Pathol. Anat.) 352: 61 (1971).
5. Clasen, R. A., et al. Electron microscopic and chemical studies of the vascular changes and edema of lead encephalopathy. Am. J. Pathol. 74: 215 (1974).
6. Goldstein, G. W., Asbury, A. K., and Diamond, I. Pathogenesis of lead encephalopathy: uptake of lead and reaction of brain capillaries. Arch. Neurol. 31: 382 (1974).
7. Kober, T. E., and Cooper, G. P. Competitive action of lead and calcium on transmitter release in bullfrog sympathetic ganglia. In: Annual Report, Center for the Study of the Human Environment, Dept. of Environmental Health, College of Medicine, Univ. of Cincinnati, Cincinnati, Ohio (1974-1975).
8. Camus, J. Toxicite des sels de plomb sur les centres nerveux. Leur periode d'incubation C. R. Soc. Biol. 68: 509 (1910).
9. Camus, J. Meningite et intoxication saturnine. C. R. Soc. Biol. 72: 861 (1912).
10. Popow, N. Ueber die Veränderungen im Rückenmarke nach Vergiftung mit Arsen, Blei, und Quecksilber. Arch. Pathol. Anat. 93: 351 (1885).
11. Weller, C. V. Tolerance in respect to the meningocerebral manifestations of actue and subacute lead poisoning. Arch. Intern. Med. 39: 45 (1927).
12. Karnovsky, M.J. A formaldehyde-glutaraldehyde fixative of high osmolality for use in electron microscopy. J. Cell Biol. 27: 137A (1965).
13. Graham, R. C., and Karnovsky, M. J. The early stages of absorption of injected horseradish peroxidase in the proximal tubules of mouse kidney: ultrastructural cytochemistry by a new technique. J. Histochem. Cytochem. 14: 291 (1966).
14. O'Tuama, L. A., et al. The distribution of inorganic lead in guinea pig brain and neural barrier tissues. Observations in control and lead poisoned animals. Toxicol. Appl. Pharmacol. (in press).
15. Delves, H. T. A micro-sampling method for the rapid determination of lead in blood by atomic absorption spectrophotometry. Analyst 95: 431 (1970).
16. Ediger, R. D., and Coleman, R. L. Modified Delves cup atomic absorption procedure for the determination of lead in blood. Atomic Absorption Newsletter 11: 33 (1972).
17. Brightman, M. W., and Reese, T. S. Junctions between intimately apposed cell membranes in the vertebrate brain. J. Cell Biol. 40: 648 (1969).
18. Roy, S., et al. Ultrastructure of cerebral vessels in chick embryo in lead intoxication. Acta Neuropathol. (Berl.) 30: 287 (1974).
19. Bull, R. J., et al. Specificity of the effects of lead on brain energy metabolism for substrates donating a cytoplasmic reducing equivalent. Environ. Health Perspect. 12: 89 (1975).
20. Nathanson, J. A., and Bloom F. E. Lead-induced inhibition of brain adenyl cyclase. Nature 255: 419 (1975).
21. Hoffman, N. E., and Weber, L. J. Increased brain calcium levels induced by an acute dose of lead in the rat. Fed. Proc. 32: 262 Abstr. (1973).
22. Cooke, W. J., and Robinson, J. D. Factors influencing calcium movements in rat brain slices. Am. J. Physiol. 221: 218 (1971).
23. Rasmussen, H. Cell communication, calcium ion, and cyclic adenosine monophosphate. Science 170: 404 (1970).